International Journal of Disaster Risk Reduction 103 (2024) 104319

Contents lists available at ScienceDirect

International Journal of Disaster Risk Reduction

journal homepage: www.elsevier.com/locate/ijdrr

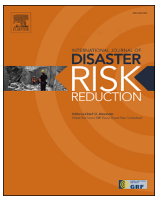

Automated geovisualization of flood disaster impacts in the global South cities with open geospatial data sets and ICEYE SAR flood data

Ohto Nygren [a, *], Mikel Calle [b], Carlos Gonzales-Inca [a], Elina Kasvi [a], Niina Käyhkö [a]

[a] Department of Geography and Geology, Geography Division, University of Turku, Turku, Finland
[b] Department of Geodynamics, Complutense University of Madrid, Madrid, Spain

ARTICLE INFO

Keywords:
Disaster risk reduction
Flood
GIS
Python
Earth observation
Open data

ABSTRACT

Flooding is a highly destructive natural disaster affecting millions of people annually, causing substantial global economic losses. Especially in the Global South, vulnerable populations with limited resources for flood protection and recovery suffer the most. However, effective flood impact analysis and standardized geospatial data processing and visualization is lacking, hindering effective disaster risk reduction. This study employs Python to develop a standardized, automated analysis and visualization model to address flood impacts after a high magnitude event anywhere in the world by using global geospatial data sets.

In order to test its applicability two relevant cases, with different locations and scales, were selected, (Bangkok, Thailand, and Tula de Allende, Mexico). In both cases the automated flood model efficiently processed flood extent and depth data from ICEYE SAR images, added the population estimates from the German Aerospace Center, and key infrastructure elements from OpenStreetMap. The output of the automated process is presented as web-based interactive maps, offering insights into flooding severity and impacts with minimal user input. This quick approach (processing time between 41 s and 10,5 min) facilitates timely responses by first responders, with great potential to aid and improve the efficiency of international humanitarian efforts.

By leveraging global high-resolution geospatial data for local-level analysis, this study demonstrates the versatility and time-saving benefits of this automated analysis and visualization. Automated models standardize results, minimizing human errors, and enabling consistent historical flood data comparison. Even though the databases are gathered from trusted sources, additional evaluation of uncertainties of the results with field data should be considered in further development of this tool. Nevertheless, this research highlights the worldwide potential, and especially the Global South, of automated global geospatial analysis to improve disaster impact reduction by enhancing efficient response efforts.

1. Introduction

Flood hazards and mismanaged flood risks have devastating economic, social, and environmental consequences particularly in rapidly growing cities of the global South. This is largely due to poorly built urban infrastructures combined with lack of up-to-date information of the risks and capacity to manage risks in a holistic manner [1]. Due to climate change floods have become more fre-

* Corresponding author.
E-mail address: ohto.nygren@gmail.com (O. Nygren).

https://doi.org/10.1016/j.ijdrr.2024.104319
Received 30 October 2023; Received in revised form 7 February 2024; Accepted 8 February 2024
Available online 16 February 2024

quent, intensive, and less predictable than before, affecting especially the poorest and most vulnerable areas in the world [2–6]. According to the Swiss Re Institute, floods caused economic losses accounting for more than 82 billion USD globally in the year 2021. Economic losses are particularly important in the Global South where only 7% of losses are covered by insurance [7]. In 2022 floods resulted in the deaths of 7954 people worldwide, significantly over the average of 5195 yearly deaths in the previous 19 years (Centre for Research on the [8]).

A significant improvement for the reduction of flood induced damages can be achieved if flood situation analysis is provided at sufficient spatial accuracy and speed to enable targeting of the first responders and humanitarian aid [9]. Flood situation analysis for operative first aid actions require a combination of multiple sources of location-specific (geospatial) information, including extent of the flooded area, estimation of the flood depth within inundated areas and sufficiently accurate data of physical infrastructures, population distribution and accessibility to different sites for mitigation actions [10–12].

Digital location-specific data sets of these critical factors can be efficiently combined, analyzed, visualized, and automated using Geographical Information Systems (GIS), AI, machine learning and coding languages such as Python [10,13,14]. However, one major challenge has been a lack of sufficiently accurate and up-to-date geospatial data of the floods and cities' key infrastructures, which are relatively scarcely available in the rapidly changing cities of the world [15]. This concerns especially combining flood extent and depth information with identification of most vulnerable informal settlements within a city, at hyper-local scales [16–20]. Another challenge has been to identify such data generation and flood situation assessment mechanisms, which would be repeatable, transferable, and scalable for disaster risk reduction efforts throughout the world, without losing a precision of local accuracy and context of flood-related information. At best, operative solutions are able to combine scalable and accurate data products, such as those generated from Earth observation satellites to ensure that flood risk assessment can be made against up-to-date situation awareness [14]. These data need to be merged into visual products, which allow fast and reliable interpretation of and responses to the situation at hand.

Recent developments of new satellite platforms and sensors with substantially improved spatiotemporal resolutions have opened new possibilities for mapping and tracking natural hazards at operational and at local scales. Synthetic-aperture radar (SAR) satellite data has become a prominent source of rapid and instantaneous assessment of flooding extent and depth due to multiple advantages compared to optical satellite imagery [21–27]. SAR sensors can penetrate cloud cover and are not affected by the lack of daylight and can thus be operated day-and-night in any weather [22]. In addition, integrating SAR data into automated processing protocols to extract fast and accurate water layers, e.g., water layer extraction in 9 min and 96% accuracy using RADARSAT [23], increases its potential use in flood related applications. The European Space Agency (ESA) offers free SAR data through its Sentinel-1 satellite constellation. Sentinel-1 SAR satellites are capable of producing data at a spatial resolution of up to 5 m with a daily revisit rate of 6 days [28,29].

Multiple novel approaches, which combine local and global data have also been co-developed and piloted to improve availability and access to local geospatial hazard and risk data of flood events, urban infrastructures, and population distribution for disaster risk reduction efforts. These include, for example mapping of global population distribution [30], crowdsourcing mapping of the effects of devastating earthquakes and other emergencies [31,32], community mapping efforts of flood risks and experienced pluvial floods [15], mapping urban floods based on social media data [33], settlement mapping using satellite imagery [34], mapping events in near-real time with aerial imagery [35], and machine learning for rapid extraction of flood extents from earth observation data [14]. Volunteered GIS campaigns and innovative student-community driven risk data collection efforts, such as those implemented in Tanzania by the Resilience Academy [36], have shown how efficiently and extensively globally open data resources, such as OpenStreetMap (OSM) can be improved and local open-access data ecosystems for climate resilience can be generated with local efforts [37].

Humanitarian aid agencies and emergency management personnel work around the clock during times of crisis to rapidly collect, verify, process, and analyze data in order to generate up-to-date situational awareness information to be used by first responders and long-term humanitarian aid operations [38,39]. Every minute saved between data processing and interpretation of results by humanitarian agencies, emergency personnel and first responders could save numerous human lives and reduce infrastructure damage. Although data accessibility and solutions for combining global and local data sets have substantially improved, there is a lack of automated and spatially explicit solutions, which would make flood situation analyzes cost-effective and reliable to support decision-making and action on the ground. Automated geovisualizations of flood impacts would increase the efficiency of the first responders when making impact assessment and action plans for aid distribution [11,40]. For any automated solution, it is important to clean up and visualize data sets into standardized, easy-to-understand and informative packages, especially in times of crisis, and to avoid visually overloaded maps that do not follow basic cartographic principles [9,41].

The aim of this study is to develop and pilot an automated, standardized, repeatable and scalable geovisualization model, which depicts possible impacts of floods on the residents of cities residing within inundated areas. Our model combines geospatial data sets of flood extent and depth with population distribution and building footprints at a local city scale to depict variation of flood impacts within a city. The model combines flood extent and flood depth information generated from the SAR satellite data space of ICEYE with globally open, yet spatially accurate geospatial data of population distribution from World Settlement Footprint (WSF) provided by the German Aerospace Center (DLR), and OpenStreetMap (OSM) data to link the flood and population information to essential services and the number of inundated buildings based on the building footprints. We will test the developed and automated model in two study cases, Bangkok (Thailand) and Tula de Allende (Mexico) to demonstrate how globally open OSM and WSF data sets in combination with flood extent and depth estimates derived from SAR satellite data can be turned into locally relevant information, which could be used as a timely action and decision-support for First Response efforts anywhere in the world. We will discuss the value of the model for possible operative applications and critically assess the methodology and challenges related to data sets and model per-

formance. Our research is based on cooperation under Resilience Academy between the University of Turku, the World Bank, DLR and ICEYE, with an objective of testing scalable flood impact geovisualization solutions for operative uses in the global South.

2. Data and methods

2.1. Data sets and study cases

The automated geovisualization model was developed using a set of geospatial packages in Python and Kepler.gl to automatically access, edit, analyze, and visualize flood disaster impacts within both study cities on a neighborhood-scale. Three high-accuracy geospatial data sets were used to develop the model. Firstly, estimates of the flood extent and depth were provided by ICEYE based on their SAR data set (Table 1). SAR imagery -based data products of ICEYE allow near real-time and high-accuracy data to monitor floods anywhere in the world [42]. Secondly, population distribution was taken from the WSF2019 data set, and thirdly building footprints and locations of essential services were derived from OpenStreetMap (OSM).

Bangkok and Tula de Allende were selected as case study cities. Both cities have a frequently flooding river running through the city and they suffered from severe fluvial and pluvial flooding during the recent years. Both cities also have key characteristics of climate risk prone cities of the global South with rapid urbanization, poorly maintained urban infrastructure and diverting flood waters from rich neighborhoods towards poorer ones [47–49]. They are also located within globally historical and projected flood risk areas [50]. However, the selected cities are also different from each other in the sense that Bangkok is a mega-city with a population of 10.9 million inhabitants and it is financially, culturally, and politically the most influential and important city in Thailand. Meanwhile Tula de Allende is a relatively modest sized city, with a population of ~115,000 inhabitants and it is mainly known for its large archeological site. These similarities and differences allow better testing of the model performance and practical value.

2.1.1. SAR-based flood extent and depth data set

The spatial flood extent and depth data layers were provided as ready-made data products of the ICEYE company. Synthetic-Aperture Radar (SAR) -based datasets depict flood inundation situations of August 2021 in the case study cities (Table 1, Fig. 2). The data was preprocessed by ICEYE by extracting flood depth values from raw SAR data and converting these into GeoTIFF data layers (Table 1). Pixel values in the delivered GeoTIFF equal flood depth in meters. No data values have been filtered out in the Python script produced in this article.

According to ICEYE, there is generally a mean absolute error (MEA) of 24–32 cm on the water depth estimations derived from ICEYE SAR data depending on the location characteristic and the quality of the DEM data used in the processing [51]. The major advantage of ICEYE SAR flood data is the persistent monitoring capability of their fleet with daily coherent ground track repeat capabilities [43,52,53]. This allows monitoring rapidly changing urban floods daily and the possibility of tracking the changing situation with identically visualized flood maps. The data is classified as near real time as there is still a rigorous pre-processing phase any SAR data has to go through which lasts a minimum of ~24 h, but this is unavoidable and sufficient for rapid mapping purposes.

2.1.2. Population distribution estimates from the World Settlement Footprint (WSF) 2019 data

Population distribution estimates of the cities were obtained from the World Settlement Footprint 2019 Population data set (WSF2019-Pop) of the German Aerospace Center (DLR) (Table 1). By request, they have created two new, improved raster data sets, which cover the study areas. This data is planned to be released globally once finished. The WSF2019-Pop data has been produced by creating a global imperviousness raster with a 10-m spatial resolution and calculating an estimated population count for every pixel

Table 1
Geospatial data sets used in the development of the automated geovisualization model of flood impacts.

Data set/variable	Source	Format	Availability	Accuracy/Precision	CRS	No-Data (raster)/ Geometry (vector)	References
Flood spatial extent and depth data	ICEYE SAR	GeoTIFF	Bangkok, Thailand	Horizontal: 30 m × 30 m Vertical: 24–32 cm Temporal: August 2021	EPSG: 32647	3.40282e+38	[43–45]
Flood spatial extent and depth data	ICEYE SAR	GeoTIFF	Tula de Allende, Mexico	Horizontal: 3 m × 3 m Vertical: 24–32 cm Temporal: August 2021	EPSG: 6369	3.40282e+38	[43–45]
WSF2019-Pop	The German Aerospace Center	GeoTIFF	Global	Horizontal: 10 m × 10 m	EPSG: 4326	n/a	[46]
Building footprints	OSM	GeoDataFrame	Global	Precise, but incomplete	EPSG: 4326	MultiPolygon, Point	https://www.openstreetmap.org/#map=3/37.86/14.41
Essential services (Hospitals & pharmacies)	OSM	GeoDataFrame	Global	Precise, but incomplete	EPSG: 4326	Multipolygon, Point	https://www.openstreetmap.org/#map=3/37.86/14.41

based on global population data from the WorldPop Global Project and data provided by the Center for International Earth Science Information Network (CIESIN) [46].

The WSF data has been validated against 900,000 validation samples by using crowdsourcing photo interpretation of very high-resolution Google Earth imagery [54]. Resilience Academy students were used extensively for the validation work in Tanzania.

2.1.3. Building footprints and service data from the OpenStreetMap (OSM)

The OpenStreetMap (OSM) data layers downloaded include all inundated building footprints, all inundated hospitals and all inundated pharmacies as discussed in more detail in the next chapter. OSM is an interactive and citizen-science generated web map and at the same time it is the most extensive open-source geospatial database in the world [55]. OSM is considered a valuable source of information that is used by NGOs and the United Nations in humanitarian aid and disaster response efforts [56–59].

OSM data layers were extracted from the study area using area of the interest polygons calculated in the script and the OSMnx Python package ([60]; Table 1; Fig. 1).

2.2. Geovisualization model design with Python

The geovisualization model was made around needs addressed in the Resilience Academy cooperation between the University of Turku, ICEYE, the World Bank and the DLR. The different data sets explained above were combined to produce a tool for effective and operative flood monitoring and action planning [37,61].

The resulting geovisualization model is an interactive, locally hosted flood impact map depicting inundated areas of different flood depths. It provides statistics of the estimated population affected by the flood waters of these areas and is repeatable anywhere in the world without any user interaction needed.

The automated geovisualization script was made using Python coding language version 3.9.0 of Python (Fig. 1). The Python script uses several open-source libraries, geospatial packages (Table 2) and the Python script was written and run using JupyterLab.

The flood spatial extent and depth raster data from ICEYE was first read into JupyterLab and reprojected to the World Geodetic System (WGS84, EPSG:4326) coordinate reference system (CRS). The raster cell size remained unchanged. The continuous raster data of the flood depth estimated by ICEYE was classified into four flood depth classes:≤35 cm, 35–50 cm, 50–100 cm, and >100 cm. The classified raster layer was then converted into vector polygons for additional processing. The floodwater depth classes were chosen based on global depth-damage curves which point to the fact that at around ≥0.5 m of floodwater depths buildings start to suffer critical structural and interior damage and it is dangerous for most people [62,63]. A slightly higher value than the MEA of ICEYE was chosen as the smallest depth class to highlight areas where there is at least some water even with an error of 32 cm in the data and

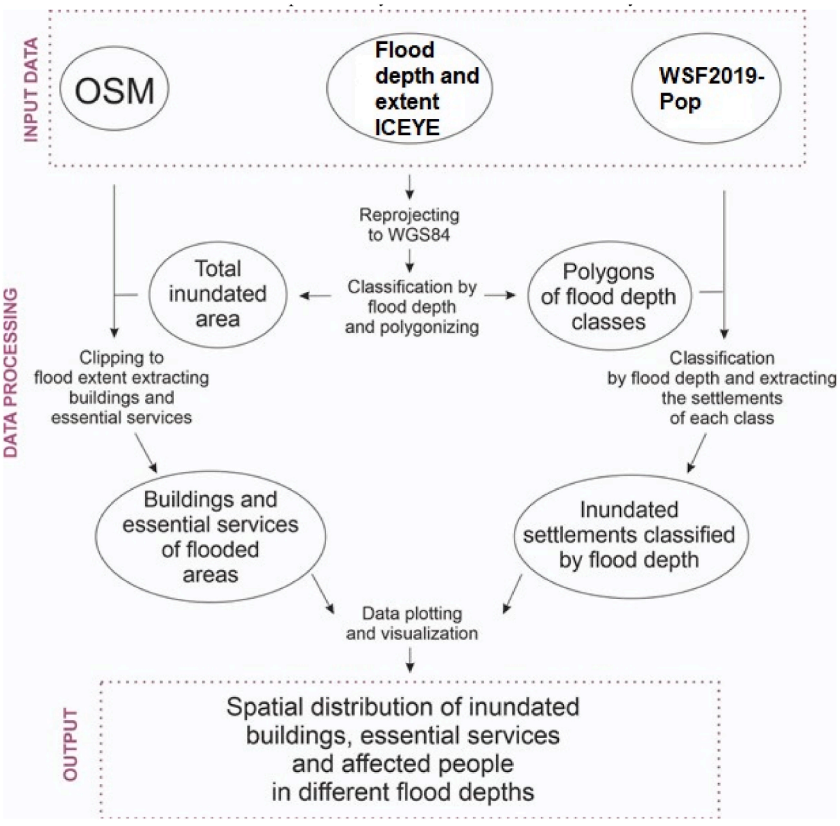

Fig. 1. The overall geovisualization model and the processing flow of the data sets and variables with the Python code.

Table 2
A list of Python libraries, packages, and modules that were used in the analysis.

Name	Version	Information
Pandas	1.4.1	https://pandas.pydata.org
Geopandas	0.10.2	https://geopandas.org/en/stable/
Matplotlib	3.4.2	https://matplotlib.org
Kepler.gl	0.3.2	https://docs.kepler.gl/docs/user-guides
Shapely	1.8.1.post1	https://shapely.readthedocs.io/en/stable/
OSMnx	1.1.2	https://osmnx.readthedocs.io/en/stable/
Rasterio	1.2.10	https://rasterio.readthedocs.io/en/latest/
PyCRS	1.0.2	https://github.com/karimbahgat/PyCRS
Os	–	https://docs.python.org/3/library/os.html
Mapclassify	2.4.3	https://pypi.org/project/mapclassify/
Seaborn	0.11.2	https://seaborn.pydata.org
Pyproj	3.3.0	https://pyproj4.github.io/pyproj/stable/
Utm	0.7.0	https://pypi.org/project/utm/

floodwaters over 1 m in depth make it extremely hard for adults to stand in and thus a danger for almost all people especially if the water is flowing even at a slow pace [64].

A Python function (“*findtheutm”, see code in GitHub*) was used to get accurate area calculations of flood extents. This was achieved with a function that takes latitude and longitude points from the centroid of the chosen data and then calculates in which UTM zone the latitude point is in and chooses the correct Coordinate Reference System (CRS) for the area calculation. The result is then converted to km^2. Using this function, the script can automatize an area calculation anywhere on Earth with minimal distortion.

To automate access to OSM freely available data from the flooded areas, the OSMnx Python package was used. Specifically, the OSM's building footprint data was downloaded using polygon masks created from the polygonized flood data to get data only from within the boundaries of the flooded area (see Appendix 1, page 4). This makes processing more efficient as data of buildings unaffected by flooding is not downloaded. The Python script gets the geographical location information and the correct coordinate system from the reprojected version of the original raster file provided by ICEYE (Fig. 2).

Unnecessary OSM data were removed and only the polygon footprints of buildings were kept. In addition, unnecessary data columns were also removed and only the “geometry”, “building”, and “name” columns were kept. The hospital and pharmacy and other public service data were also extracted as point features and used to highlight their location to avoid duplicate building polygons.

The hospital and pharmacy data had to be searched for using two different OSM tags since OSM data can be mapped in different ways depending on which tags the editing user decides to use. Each OSM element has a tag that consists of a key and a value. The tags describe OSM elements; the key (the column name) describes the topic, category, or type of feature and the value provides detail for the key-specified feature. For example, the hospitals were searched for using the tags “building = hospital” and “amenity = hospital” and to find all the inundated buildings the tag “building = True” was used.

Overlay analysis and zonal statistics (using Rasterio package function) of the vector and raster data was used to achieve results on the impact of the floods. For example, the flood depth class data was overlaid on top of the WSF2019-Pop and OSM building footprint data to generate a flood damage map and to find out how many people lived in areas affected by different water depths and how many buildings had been inundated by the floodwaters. This method not only returns a statistical report of the total population affected by a flooding event but also divides it by flood damage severity classes to reveal the number of people affected by extreme water depths and thus in dire need of immediate assistance.

2.3. Geovisualization of the flood impacts with Kepler gl

Kepler.gl is a high-performance open-source web-based application for visualizing large geospatial data sets [65]. It is built on top of Mapbox GL and deck.gl which are services that provide custom online maps and complex visualizations possibilities. Kepler.gl is able to render millions of data points on the fly and performs very well with large data sets. Creating a map in JupyterLab by using the

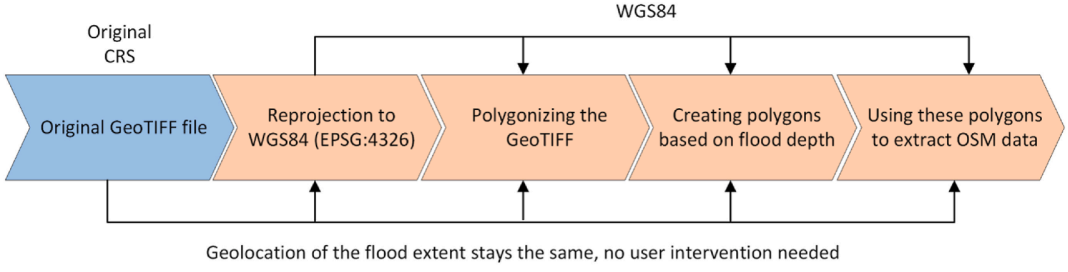

Fig. 2. Flowchart depicts how the geovisualization model locates the correct area of interest based on the ICEYE flood data layer to download OSM data variables (building footprints, services), removing a need for human intervention.

Kepler.gl library allows the user to add data with a few lines of code and opens an interactive view of Kepler.gl where it is possible to edit the visualization. Icon names for hospitals and pharmacies had to be inserted into new columns in the corresponding GeoDataFrames ('plus-alt' for hospitals and 'heart' for pharmacies) so that these string values could then be recognized by Kepler.gl to import them from the Kepler.gl icon database. Once satisfied with the visualization the configurations can be saved as a variable (variable named "config" in this script) and used with other data that is named exactly the same and is in the same format. The Kepler.gl map visualizations can also be changed while viewing the maps, but these changes are not saved. To save edited visualizations for later use, the user has to edit the configurations, call the configurations with the "map.config" function, and save the configurations as a variable in the script.

In this script, ICEYE flood depth data, WFS2019-Pop, and OSM data (inundated buildings, hospitals, and pharmacies) were added to a Kepler.gl map and then visualized using the Kepler.gl configurations. Latitude and longitude values extracted from the flood extent data were used to zoom the map to the flooded area. The maps from Bangkok and Tula de Allende were then saved as local HTML files which can be opened with a web browser if the file is downloaded to the computer in use. This was done because Kepler.gl is a client-side only application, which means that it does not send or store any data to any backends, limiting the saving and sharing of maps. The advantage of saving the map as an HTML file is that once downloaded it can be viewed and used normally by opening the file with a web browser. The map can also be shared by sending just the HTML file to another user. The script also exports a bar chart of the amount of population affected by different flood depths as well as prints out text of the number of hospitals, pharmacies and buildings inundated. This data can then be shared as an image and as text.

3. Results

3.1. Code and performance of the automated geovisualization model

The developed code met all requirements previously set for its use as a tool for fast reacting after flood events in both study sites. The code can be found in the following GitHub repository: https://github.com/resilienceacademy/-flood-automapping. The data outcomes from the automated model consistently mapped the two study sites to the correct location despite the different coordinate reference systems (CRS) in the source data. This means that the reprojection process in the code works automatically without the user having to worry about projecting the data correctly. The area calculations are also accurate, despite the geographic location of the flood changing as the "*findtheutm*" function finds the correct CRS to use for the area in question The final map also automatically zooms to the correct area of interest without user interaction.

To evaluate the performance of the model in these two case study areas a series of test sets were carried out (Table 3). The longest processing time (7 min 40 s) corresponded to the Bangkok metropolitan area. This was related to the model step where it extracts the over 12,000 building footprints of the inundated buildings in the study site. As there were only 36 building footprints in the flooded area in Tula de Allende, it took only 12.86 s on average to extract the data. There is a significant difference in the total average processing time between the two study areas with 10 min and 33 s for Bangkok and only 41.73 s for Tula de Allende. This is logically explained easily by the difference in the flood extent, 718.76 km^2 in Bangkok and only 2.2 km^2 in Tula de Allende, and thus also the difference in the amount of OSM data from these two areas. The visualization configurations in Kepler.gl transfer over without issue and as such the visual look of the flooding events are identical in both study sites.

Table 3
Processing times during each testing round of the script, and averages for both study areas. The script performed consistently in the 5 test runs per study area.

	Time in seconds (Bangkok, Thailand)					
Process	1st test	2nd test	3rd test	4th test	5th test	Average
Importing modules	8.21	7.92	7.3	6.03	4.39	6.77
Raster transformations	0.846	0.776	0.571	0.62	0.272	0.617
Vector transformations	108	95	90	91	89	94.6
Raster clipping	27	25.7	27.3	26.3	25.7	26.4
Getting OSM data	492	460	453	456	441	460.4
Results	26.2	25.3	26.3	26.6	24.7	25.82
Kepler.gl	32.6	14.073	15.193	15.176	16.065	18.621
Total time	694.856	628.769	619.66	621.726	601.127	633.228
	Time in seconds (Tula de Allende, Mexico)					
Process	1st test	2nd test	3rd test	4th test	5th test	Average
Importing modules	6.95	6.53	3.04	3.94	4.53	4.998
Raster transformations	0.272	0.55	0.314	0.442	0.31	0.378
Vector transformations	18.7	18.6	18.1	19.4	19.9	18.94
Raster clipping	1.24	1.15	1.35	1.14	1.64	1.304
Getting OSM data	21.8	10.2	10.2	11.3	10.8	12.86
Results	1.71	2.00	1.98	2.42	2.55	2.132
Kepler.gl	1.525	1.338	0.962	0.882	0.93	1.127
Total time	52.197	40.368	35.946	39.524	40.660	41.739

3.1.1. Model sensitiveness

The results of the model are very sensitive to the data used, as are all models. The datasets chosen for this study have been vetted by previous studies and have been found to be accurate as described in section 2.1. The modeling results sensitivity to the input data was tested and illustrated by running the model with alternative population data layers.

Running the model in Tula De Allende with Global Human Settlement Layer (GHSL) and WorldPop population data returns almost the same result for people affected by the flood: 6637 for the GHSL data and 6522 for the WorldPop data. This is significantly more than the result of 4908 people affected based on the WSF2019-Pop data. This can be attributed to the significantly larger cell size of the GHSL (250 × 250 m) and WorldPop (100 × 100 m) data which causes overlap with the actual riverbed and the data grids (Fig. 3.) The significantly more accurate WSF2019-Pop (10 × 10 m) data shows no values on top of the actual riverbed as it is not inhabitable. Population data grids which are too large cannot properly mode intricate cities built around flood prone rivers causing estimates of the affected population to be exaggerated. In the Global South these areas are where the most vulnerable populations live.

The accuracy of the analysis created by the model is also very sensitive to the availability and quality of OSM data in the region. Comparing the results of inundated buildings to satellite imagery highlights the fact that only a fraction of the buildings in Tula de Allende have been mapped to OSM (Fig. 4). The same can be observed in the map created from Bangkok, Thailand. OSM data, however, is constantly changing and the results will be better in the future as the OSM project is ongoing.

3.1.2. Geovisualization outputs of flood impacts in the case study cities

The results generated by our model are produced in the exact same format for both case study cities and there are no issues with area calculations as the model can choose the correct Universal Transverse Mercator (UTM) zone for each data set and perform the area calculations based on the location of the flood globally.

The geovisualizations from Bangkok and Tula de Allende produced by the model script can be viewed by going to: https://drive.google.com/drive/folders/1UPXMbsMnxtNXkGiR3bTDE3495XTZqCne and downloading the to.html files and then opening them in a browser. The files should open in the default browser where the user can then interact with the maps.

Based on our modeling results the total flooded area in Bangkok (718.76 km^2) covered an area where over 13,000 buildings were inundated with floodwater threatening 1.4 million people (Fig. 5.). The equivalent numbers in Tula de Allende (~2.20 km^2) were 36 buildings, with nearly 5000 people living within inundated areas (Fig. 6).

A more careful examination of the population estimates against the depth of the flood shows that in Bangkok, Thailand 685,989 live in areas that were inundated by over 0.5 m of water, which indicates that their buildings were severely inundated. The flooding in August of 2021 in Bangkok, Thailand was so extensive that 1,013,859 people were living in areas that had estimated flood depths

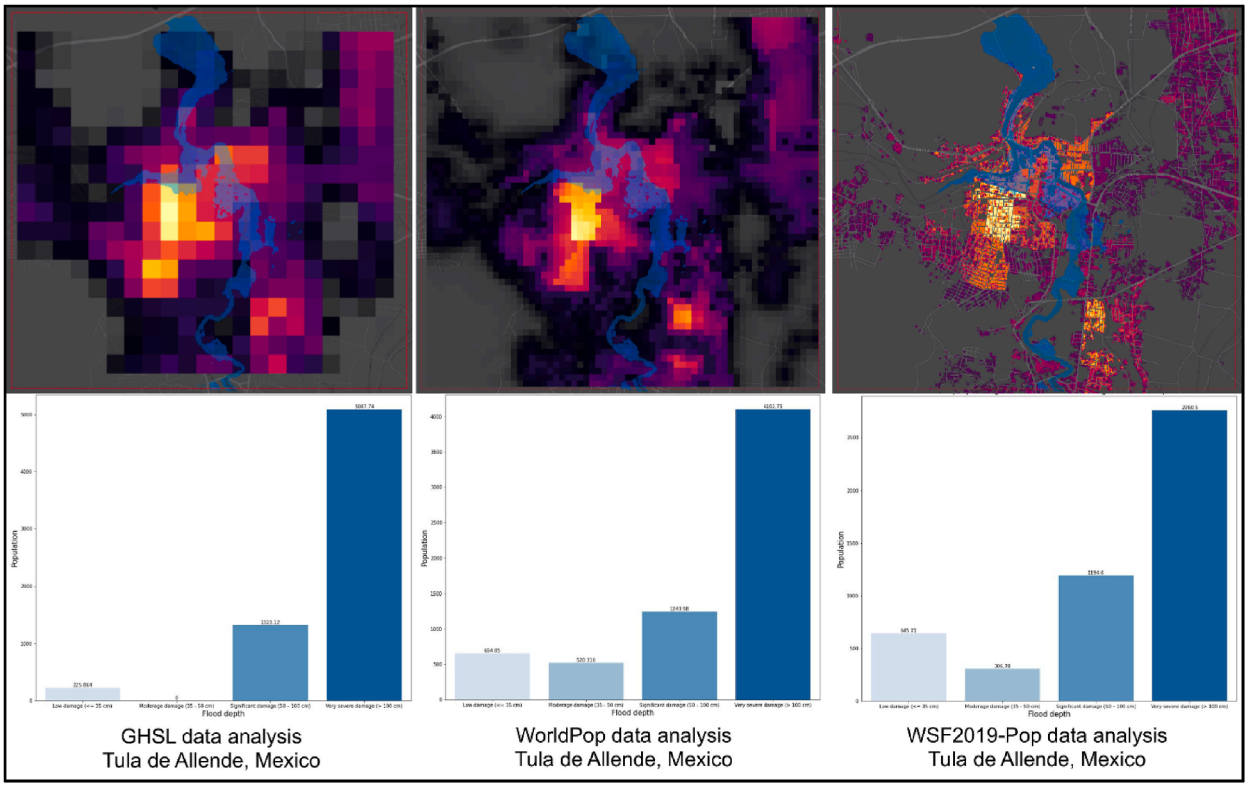

Fig. 3. Model analysis of Tula de Allende using three different population datasets: GHSL, WorldPop and WSF2019-pop data. The analysis shows the significance of high precision datasets as too large raster cell sizes exaggerate the number of people affected.

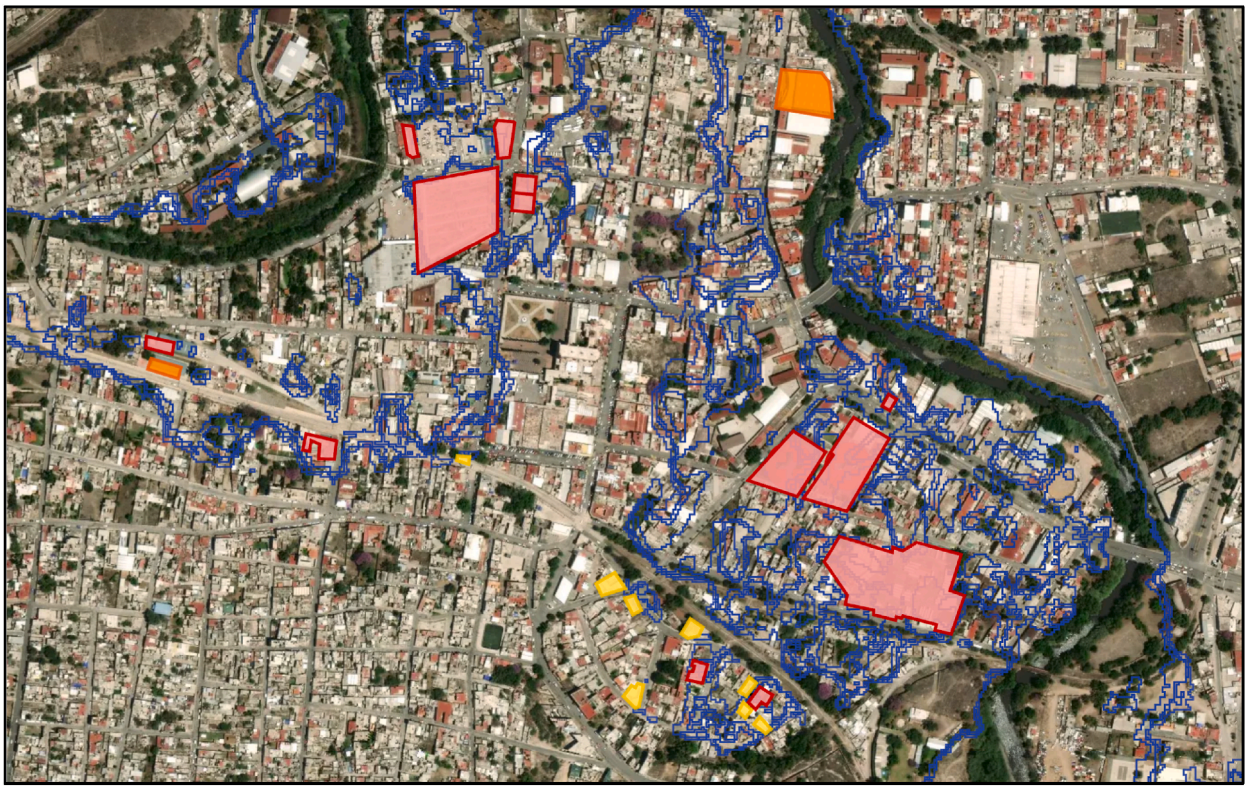

Fig. 4. Snapshot of the flood in Tula de Allende. The blue lines show the outlines of the flooded areas, and the red, orange and yellow polygons show flooded building footprints of the OSM data set. The image highlights the immense lack of OSM data in the area. Satellite imagery by Mapbox.

of over 0.25 m during the flooding event. The people severely affected most likely had little or no chance to go outside during this flooding event and the water levels that were captured and estimated by the ICEYE flood depth and extent data would have caused first responders significant trouble to reach these people in urgent need of assistance.

According to the overlay analysis of the flooded area, there were 5112 buildings inundated by over 0.5 m of water, 6260 buildings inundated by a maximum of 0.5 m of water, and 1786 buildings that fell in-between the two categories, bringing the total number of inundated buildings to 12,843 based on the OSM data during the writing of this article. Of these buildings, 75 were hospital buildings and 11 were pharmacies. This does not mean that 75 separate hospitals in Bangkok were inundated as hospitals usually consist of multiple separate buildings. Most of the mapped buildings in OSM in the area of Bangkok are strategically, societally, or economically important big buildings. The OSM data in the area of Bangkok lacks many buildings, which makes the situation much direr in reality, especially in the poor neighborhoods that are often overlooked in favor of mapping more affluent and economically important areas. These results might change considerably even in a short span of time as OSM is constantly changing and updating by nature.

A total of 4908 people were affected by the flooding in Tula de Allende, Mexico in August of 2021. Of these people, 3956 lived in areas that were inundated by over 0.5 m of water according to the flood classes calculated from the ICEYE SAR data. Of the 36 inundated buildings in Tula de Allende, two were hospital buildings. There were no inundated pharmacy buildings, which also proves that the script does not cause an error if there is no data from the area of interest. The OSM data in the area of Tula de Allende, Mexico lacks a majority of buildings, like in the case of Bangkok, which makes the number of inundated buildings much higher in reality. The results show a severe lack of data in these Global South cities and reveal the need to increase the pace of mapping OSM data in these areas. The results are from the time of writing as OSM data is constantly updated.

4. Discussion

4.1. Opportunities for automated geovisualization of local flood impacts with global data sets

Based on the results, the automated geovisualization model developed in this study works consistently and accelerates the flood impact assessment work in practice. The model and use of globally available, yet locally accurate geospatial data sets are capable of producing explicit information of the expected impacts of floods to the residents residing in the cities. The geovisualization shows, through the combination of multiple geospatial local scale data sets where the most severely flooded areas in the city are and how many residents are estimated to be impacted. The geovisualization model can be fairly easily modified and optimized towards specific areas/use cases by changing a few lines of the source code. The process is much faster than using desktop GIS software, although the code can also be run in ArcGIS Pro using the ArcGIS Notebooks. Even though this study focused on mapping the impact of floods, this

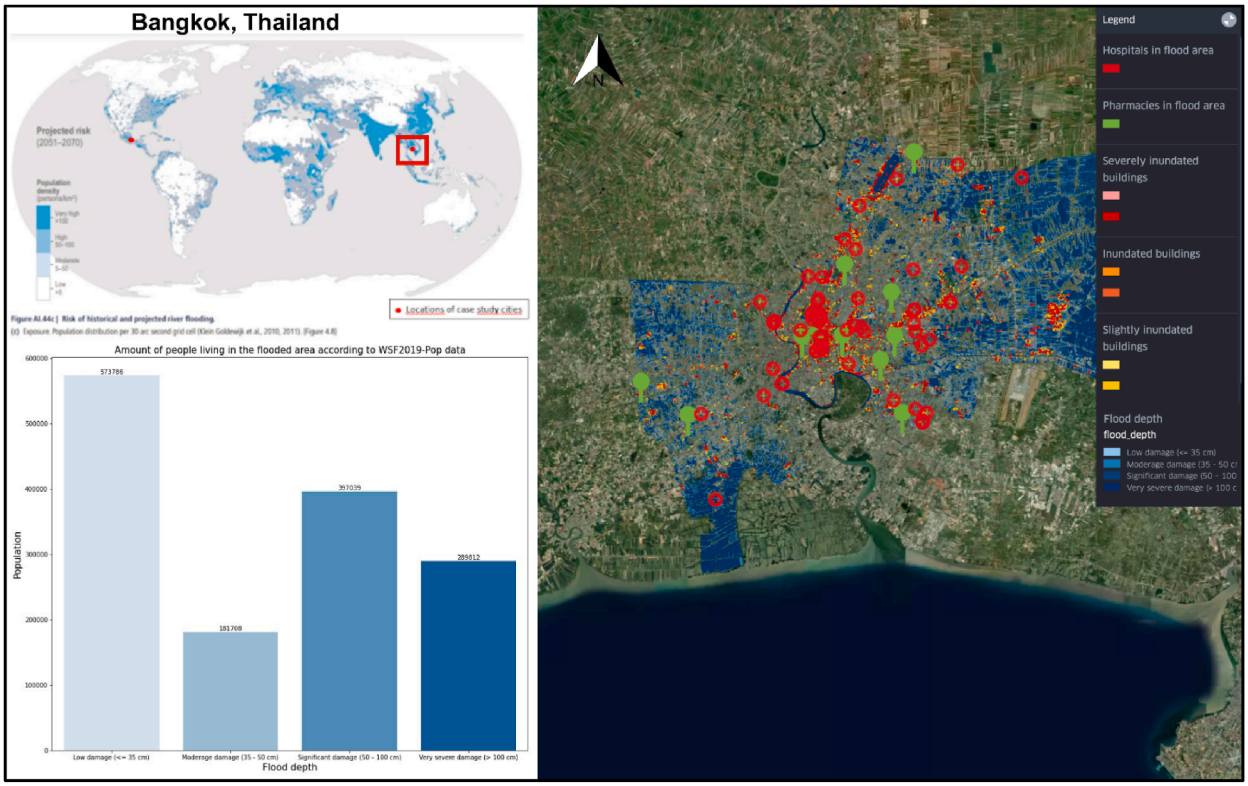

Fig. 5. Estimated number of residents affected by the floods in Bangkok, Thailand.

model can map any disasters that have been captured using remote sensing methods. The model analyzes the impact on humans and infrastructure within the area of interest and can just as well be used to map the impact of earthquakes or large-scale bombing in conflict zones. One can even use other raster data than SAR data. Only the classification of flood depth zones needs to be removed or modified to suit the use case.

To use the model, the user can download the code from the GitHub repository (https://github.com/resilienceacademy/-flood-automapping) and install all Python libraries listed in Table 2. After this the user must have access to a raster layer depicting an area of interest (e.g. METEOR project fluvial flood data in the Climate Risk Database of the Resilience Academy) and a raster layer depicting population estimates (e.g. WordPop data). The model was tested with several different population datasets (WFS, WorldPop and Global Human Settlement Layer GHSL) and flood data (ICEYE, METEOR project) and worked without any issues.

The value in the automated geovisualization model comes from the spatial and temporal accuracy, model speed and repeatability in which the visualizations are produced. For smaller cities like Tula de Allende, the map is practically instantly ready for use, and depends only on the time it takes for ICEYE to process flood extent and depth data sets. ICEYE is capable of providing SAR imagery in as little as 15 min from image acquisition [66]. To replicate the exact results of the study the model requires access to the ICEYE flood depth and extent data that has been processed from raw SAR data by ICEYE with information of the flood depth. While this model does not process and prepare raw SAR data, there are multiple different models to perform the pre-processing phase [14,27]. Connecting this model to one of the SAR processing models will speed up the front-end of the process: delivering geovisualised maps and statistics of flood impacts. This will produce financial gain as it saves the valuable working time of analysts and faster response to disasters saves lives, reduces the amount of damage caused to infrastructure and speeds up the rebuilding process [14].

The geovisualization model can run with any population data that is in a raster format, but the WSF2019-Pop data has a few key advantages. Its spatial resolution of ~10 m at the equator is much higher than other openly available global population data sets like the WorldPop data or the Global Human Settlement Layer (GHSL) data, which have a spatial resolution of 100 m. This is important when mapping flooded areas, which can be very intricate and unpredictable, especially in city environments. Using population data that is too coarse leads to overestimation of the number of most affected populations during flooding as the data overlaps the rivers and other water bodies where the highest measured flood depths often are. In times of emergency when first responders need estimates to be as accurate as possible, data that is too coarse and causes overestimations is a problem.

Maps and statistics produced by the script would be relevant for first response teams and humanitarian aid organizations since the model is considerably faster than other rapid mapping services such as the Copernicus Emergency Management Service (CEMS) and the United Nations Institute for Training and Research - Operational Satellite Applications Programme (UNITAR/UNOSAT) Rapid Mapping Service [67,68]. Several different geospatial data visualization libraries were tested aside from Kepler.gl including Folium,

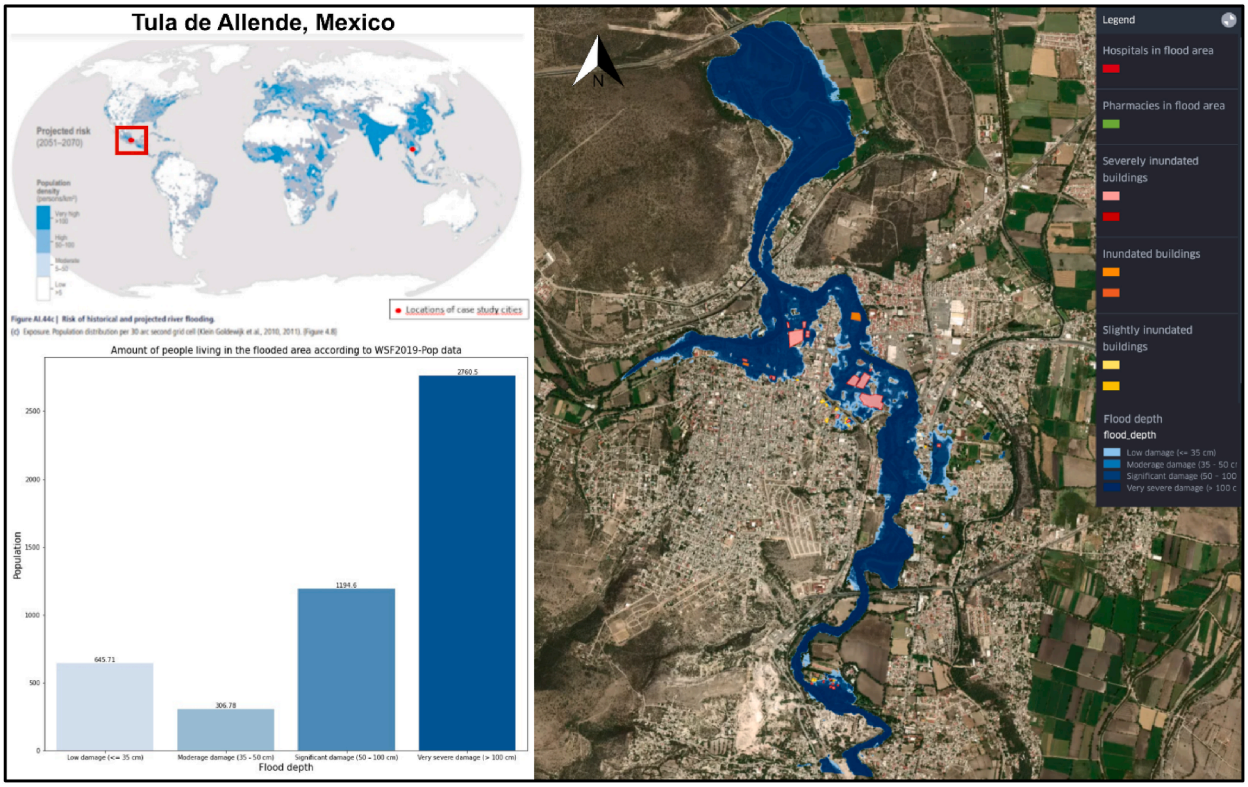

Fig. 6. Estimated number of residents affected by the floods in Tule de Allende.

Leafmap, Plotly, IpyLeaflet, and Geemap, but ultimately Kepler.gl was chosen as the most suitable for this study because it is free, it can handle a lot of data points, it offers a wide variety of visualization options and other modifications.

Using this model, the first response is more efficient and can be focused on the areas which are most in need of aid relief. Geospatial data can also be used to analyze past trends for future risk areas and to develop early warning systems for imminent floods or other disasters.

4.2. Challenges related to the use of geospatial data sets for operative cases

There are still challenges with the developed model, mainly around the possible future deprecations or compatibility issues between the different Python libraries and packages used, which raised some issues already during the process of writing the code. One function that was missing from all the Python libraries used was the ability to easily and accurately overlay raster files that have no data values. Also, the ability to upload the visualization to an online server for sharing would have been very useful, but there are so many costs involved in running a server that services with this option are subscription-based with monthly or yearly costs (e.g., ArcGIS Online).

Also, the chosen geospatial data sets and their quality, accessibility and use still have several issues of concern for wider adoption of the model for disaster risk management operations.

Firstly, mean absolute error in the ICEYE flood depth data causes uncertainties in the results of the analysis and these cannot be avoided without in-situ measurements of the actual flood depths at the same time as the SAR data is generated. Our initial cooperation plan was to evaluate in-situ calibration with SAR flood depth measurements in Dar es Salaam, Tanzania, but due to lack of floods in 2020–21, we could not materialize the plan, and thus omitted Dar es Salaam as a case study city. Lee et al [69] compared in-situ depth measurements of dam reservoirs to TDX InSAR data with a spatial resolution of 12 m and the difference between the in-situ and SAR-derived data was between ± 1 m with a standard deviation of 0.60 m. Barreto et al. [70] were also able to estimate water levels in rivers accurately with SAR data by comparing results to extensive field measurements. Charles Blanchet of ICEYE has also stated in an interview that their mean absolute error is 24–32 cm [51]. This suggests that ICEYE's estimations can be deemed plausible and fairly accurate and that SAR satellites can be used to monitor flood water depths as long as a margin of error is acceptable.

An error prediction module with ancillary data, such as high-resolution topographic data, in the geo-visualization could enhance the model and reduce uncertainties due to flood depth inaccuracy [71,72]. The flood extent data however is extremely accurate compared to similar data extracted from lower resolution Sentinel-1 SAR imagery from or satellite imagery. The approach also favors the use of ICEYE SAR data as there is no alternative in terms of accuracy and availability. This data can however be too expensive for many smaller actors and due to this the model is aimed to be used by large, global actors such as the World Bank, the UN, or the Red Cross.

Secondly, the WFS2019-Pop data however has not yet been released fully as it is still being worked on in-house at the DLR. However, the results are accurate when compared to other world population data sets and census data from the regions [46]. Using the model with existing worldwide population datasets also causes over estimations of the number of people affected as the raster cell sizes are too big in other datasets (e.g. GSHL and WorldPop) to accurately map intricate cities in the Global South where informal settlements often sprawl around extremely flood prone rivers flowing through the city.

Thirdly, OSM data is still lacking detailed data in many rapidly developing countries and cities, and this causes very high margins of error in the analysis in both Tula de Allende and Bangkok. The quality of OSM data also varies extremely from building to building and due to this only the polygon building footprints have been used in the analysis. The visual comparison of OSM data and satellite imagery shows that OSM is lacking many building footprints in both study sites. There is a severe lack of building footprints in the city centers, which are almost always the most extensively mapped due to the high concentration of economically, strategically, and socially important locations, thus data lacking from these areas suggests that most probably the situation is even worse in more peripheral rural regions [57]. This model however can be used to run the same analysis in cities with frequently reoccurring flooding and thus highlight the areas most in need of mapping. The people living in the flood risk areas are the ones most in need of help during a flood and data analysis such as the one provided by this study's model is a way to get help there as fast as possible. Mapping the flood risk areas of the Global South through services such as OSM provides a way to help and understand the risk these areas face. The mapping can be done through mapathons or by leveraging AI models to create building footprints from high quality satellite data. While using OSM data can be seen as a weakness of this model, the OSM project is not going away, and more and more data is added to OSM every single day. This model can also be used to raise awareness of the areas most in need of geospatial data to help rescue efforts and humanitarian aid. There can also be significant download times when using OSM data from extremely large floods such as the 2022 Pakistan floods. This can however be circumvented by making multiple maps, one for each municipality for example.

While there has been considerable thought put into the datasets selected for this study and the data has been evaluated and compared thoroughly, the main value of the model, however, comes from automating the process and enabling the use of different data sources. This enables the user to evaluate the accuracy and completeness of datasets and use their preferred datasets for the analysis. This also enables the model to be used to evaluate all natural phenomena and human conflicts that happen within an area of interest and that have been captured using remote sensing methods such as SAR satellites.

4.3. Future development needs

Since the geovisualization model was built and published using open-source code, anyone can use it freely and develop the code further. Future developments could include uploading the data to an online web map for easier sharing, but this would require more funding to cover the costs included as there are no services providing this for free.

While SAR data provided by ICEYE is not generally free, it has many advantages compared to freely available SAR data from Sentinel-1. The less than daily revisit rate of the ICEYE constellation provides critical data when it is needed from anywhere in the world, while the Sentinel-1 constellation is only capable of a 6–day revisit cycle. The spatial resolution of ICEYE's Spot Mode is 0.25 m, which is considerably higher quality than Sentinel-1's free SAR data that has a spatial resolution of 10 m [29]. This difference in the spatial resolution is a significant factor to the quality of flood estimations in urban city environments of the Global South, which are extremely densely populated with informal settlements, a lack of building regulations and/or city master plans.

As WSF and OSM are globally open geospatial data services and products, they can also be freely used and OSM data can be actively updated with targeted mapping campaigns to ensure sufficient data quality. Adding road networks from OSM would allow them to be used in routing first response vehicles on site and to warn about roads destroyed or blocked by the flooding. The output could also be turned into a dashboard to allow the visualization of the graphs and numerical data produced by the model. Essential elements of effective and automated geovisualizations should include a scalable model with a dynamic map combined with graphs and charts which show the scope of a disaster [73].

The visual outlook should also be finalized using a panel of seasoned emergency response professionals to make sure it follows global guidelines and universally understandable symbology. Volunteered geographic information (VGI) data could also be gathered during disasters and implemented into a dashboard view in order to see people in distress and to gain insight from people on the ground.

Simultaneously, the need and utility of more open-source geospatial data can be tracked. The critical risk areas can be identified for future improvements and essential services for these areas can be planned to withstand flooding either by reinforcing the buildings, constructing flood preventative measures, increasing people's awareness of the risks, or by relocating the settlements just outside the critical risk area.

5. Conclusions

This study successfully developed an automated tool that aims to contribute to disaster risk reduction, especially helpful in the Global South. It automatically gathers global geospatial data by using the Python programming language, to produce a standardized, automated flood analysis and visualization model. The model ingests raster data of a flooding event provided by the user (commercially produced SAR satellite data by ICEYE) and combines it with global datasets such as open-source population estimation data by the German Aerospace Center (DLR) and volunteered geographic information (VGI) from the OpenStreetMap (OSM) project. Such overlay produces ready to use GIS data, statistics of the effects of a disaster caused by flooding, and an interactive map of the scope of the disaster. Thus, the model can produce analytic and descriptive data from anywhere in the world in minutes to be used by first response efforts and global humanitarian aid.

In particular, this study highlights that global data sets can be used to achieve significant and extremely important data visualizations in a timely manner when the process is automated through coding, in this case with Python language. Automating the analysis and visualization of the data considerably speeds up production of relevant data visualizations and frees up resources of GIS analysts. However, it also points out that the main obstacles to success are related to the accuracy, availability, and cost of the data when relaying into commercial products.

Finally, the model created in this study can be effectively used to create the first assessment of a flooding event anywhere in the world but, as pointed out before, it may be greatly enhanced when combined with collaborative efforts with both global and local stakeholders. Therefore, future development of this tool, combined with site specific collaborations, shall provide the newest, most efficient technology and methods, while taking into consideration the complex needs and concerns of local inhabitants most affected by natural disasters.

CRediT authorship contribution statement

Ohto Nygren: Conceptualization, Data curation, Formal analysis, Investigation, Methodology, Resources, Software, Validation, Visualization, Writing – original draft, Writing – review & editing. **Mikel Calle:** Conceptualization, Methodology, Writing – original draft. **Carlos Gonzales-Inca:** Conceptualization, Formal analysis, Investigation, Methodology, Validation, Writing – original draft. **Elina Kasvi:** Conceptualization, Methodology, Validation, Writing – original draft. **Niina Käyhkö:** Conceptualization, Funding acquisition, Methodology, Project administration, Supervision, Validation, Writing – original draft.

Declaration of competing interest

The authors declare that they have no known competing financial interests or personal relationships that could have appeared to influence the work reported in this paper.

Data availability

The authors do not have permission to share data.

Acknowledgements

This study was done in cooperation between the UTU Geospatial Labs of the University of Turku and The German Aerospace Center (DLR), ICEYE Ltd., The World Bank, GFDRR and The Tanzania Resilience Academy (https://resilienceacademy.ac.tz/). We extend our sincere gratitude to our collaborators for their invaluable guidance, and provision of crucial digital datasets instrumental to our research.Declaration of competing interest.

References

[1] J. Rentschler, M. Salhab, B.A. Jafino, Flood exposure and poverty in 188 countries, Nat. Commun. 13 (2022) 3527, https://doi.org/10.1038/s41467-022-30727-4.
[2] Y. Depietri, F.G. Renaud, G. Kallis, Heat waves and floods in urban areas: a policy-oriented review of ecosystem services, Sustain. Sci. 7 (2011) 5–107, https://doi.org/10.1007/s11625-011-0142-4.
[3] D. Hyndman, D. Hyndman, Natural Hazards and Disasters, fifth ed., Cengage Learning, Boston, MA, USA, 2017, p. 540.
[4] L. Alfieri, B. Bisselink, F. Dottori, G. Naumann, A. de Roo, P. Salamon, K. Wyser, L. Feyen, Global projections of river flood risk in a warmer world Earth's Future 5 (2) (2016) 171–182, https://doi.org/10.1002/2016EF000485.
[5] K. Krellenberg, J. Welz, F. Link, K. Barth, Urban vulnerability and the contribution of socio-environmental fragmentation: theoretical and methodological pathways, Prog. Hum. Geogr. 41 (4) (2016) 408–431, https://doi.org/10.1177/0309132516645959.
[6] IPCC, Annex I: global to regional atlas, in: D.C. Roberts, M. Tignor, E.S. Poloczanska, K. Mintenbeck, A. Alegría, M. Craig, S. Langsdorf, S. Löschke, V. Möller, A. Okem, B. Rama (Eds.), Climate Change 2022: Impacts, Adaptation and Vulnerability. Contribution of Working Group II to the Sixth Assessment Report of the Intergovernmental Panel on Climate Change [H.-O. Pörtner, Cambridge University Press, Cambridge, UK and New York, NY, USA, 2022, p. 2875, https://doi.org/10.1017/9781009325844.028.
[7] L. Bevere, F. Remondi, Natural Catastrophes in 2021. Focus Flood: Building Resilience against a Rapidly Growing Risk, 2022 Sigma 1, 2022, pp. 1–28. https://www.swissre.com/institute/research/sigma-research/sigma-2022-01.html.
[8] Centre for Research on the Epidemiology Disasters, Disasters in numbers, Brussels (2022) 2022 Retrieved from https://reliefweb.int/report/world/2022-disasters-numbers.
[9] P. Meier, New information technologies and their impact on the humanitarian sector, Int. Rev. Red Cross 93 (884) (2011) 1239–1263, https://doi.org/10.1017/S1816383112000318.
[10] M.F. Goodchild, J.A. Glennon, Crowdsourcing geographic information for disaster response: a research frontier, International Journal of Digital Earth 3 (3) (2010) 231–241, https://doi.org/10.1080/17538941003759255.
[11] T.R. Petty, N. Noman, D. Ding, J.B. Gongwer, Flood forecasting GIS water-flow visualization enhancement (WaVE): a case study, J. Geogr. Inf. Syst. 8 (2016) 692–728, https://doi.org/10.4236/jgis.2016.86055.
[12] E. Nemni, J. Bullock, S. Belabbes, L. Bromley, Fully convolutional neural network for rapid flood segmentation in synthetic aperture radar imagery, Remote Sens. 12 (16) (2020) 2532. https://doi.org/10.3390/rs12162532.
[13] R. Al-Tahir, R.S. Mahabir, Applications of remote sensing and GIS technologies in flood risk management, in: D.D. Chadee, J.M. Sutherland, J.B. Agard (Eds.), *Flooding And Climate Change Sectorial Impacts and Adaptation Strategies for the Caribbean Region*, 138–150, Nova Publishers, 2014. https://www.researchgate.net/publication/261000276_Applications_of_Remote_Sensing_and_GIS_Technologies_in_Flood_Risk_Management.
[14] E. Nemni, J. Bullock, S. Belabbes, L. Bromley, Fully convolutional neural network for rapid flood segmentation in synthetic aperture radar imagery, Rem. Sens. 12 (16) (2020) 2532, https://doi.org/10.3390/rs12162532.
[15] L. Peterson, M.-C. ten Veldhuis, G. Verhoeven, Z. Kapelan, I. Maholi, H.C. Winsemius, Community mapping supports comprehensive urban flood modeling for floods risk management in a data-scarce environment, Front. Earth Sci. 8 (2020) 1–15, https://doi.org/10.3389/feart.2020.00304.
[16] S.B. Guerreiro, V. Glenis, R.J. Dawson, C. Kilsby, Pluvial flooding in European cities - a continental approach to urban flood modelling, Water 9 (4) (2017) 296, https://doi.org/10.3390/w9040296.
[17] C.M. Bhatt, G.S. Rao, S. Jangam, Detection of urban flood inundation using RISAT-1 SAR images: a case study of Srinagar, Jammu and Kashmir (North India)

floods of September 2014, Modeling Earth Systems and Environment 6 (2020) 429–438, https://doi.org/10.1007/s40808-019-00690-z.
[18] J.C. Young, R. Lynch, S. Boakye–Achampong, C. Jowaisas, J. Sam, B. Norlander, Volunteer geographic information in the Global South: barriers to local implementation of mapping projects across Africa, Geojournal 86 (2020) 2227–2243, https://doi.org/10.1007/s10708-020-10184-6.
[19] E. Falco, J. Zambrano–Verratti, R. Kleinhans, Web-based participatory mapping in informal settlements: the slums of Caracas, Venezuela, Habitat Int 94 (2020) 1–10, https://doi.org/10.1016/j.habitatint.2019.102038.
[20] S.S. Baghermanesh, S. Jabari, H. McGrath, Urban flood detection using TerraSAR-X and SAR simulated reflectivity maps, Rem. Sens. 14 (23) (2022), https://doi.org/10.3390/rs14236154.
[21] H.-W. Chung, C.-C. Liu, I.-F. Cheng, Y.-R. Lee, M.-C. Shieh, Rapid response to a typhoon-induced flood with an SAR-derived map of inundated areas: case study and validation, Rem. Sens. 7 (9) (2015) 11954–11973, https://doi.org/10.3390/rs70911954.
[22] F. Bioresita, A. Puissant, A. Stumpf, J.-P. Malet, A method for automatic and rapid mapping of water surfaces from sentinel-1 imagery, Rem. Sens. 10 (2) (2018) 217, https://doi.org/10.3390/rs10020217.
[23] S.K. Kuntla, P. Manjusree, Development of an automated tool for delineation of flood footprints from SAR imagery for rapid disaster response: a case study, Journal of the Indian Society of Remote Sensing 48 (6) (2020) 935–944, https://doi.org/10.1007/s12524-020-01125-4.
[24] M. Singha, J. Dong, S. Sarmah, N. You, Y. Zhou, G. Zhang, R. Doughty, X. Xiao, Identifying floods and flood-affected paddy rice fields in Bangladesh based on Sentinel-1 imagery and Google Earth Engine, ISPRS J. Photogrammetry Remote Sens. 166 (2020) 278–293, https://doi.org/10.1016/j.isprsjprs.2020.06.011.
[25] V. Tiwari, V. Kumar, M.A. Matin, A. Thapa, W.L. Ellenburg, N. Gupta, S. Thapa, Flood inundation mapping- Kerala 2018; Harnessing the power of SAR, automatic threshold detection method and Google Earth Engine, PLoS One 15 (8) (2020) e0237324, https://doi.org/10.1371/journal.pone.0237324.
[26] P. Tripathy, T. Malladi, Global flood mapper: a novel Google earth engine application for rapid flood mapping using sentinel-1 SAR, Nat. Hazards (2022), https://doi.org/10.1007/s11069-022-05428-2.
[27] A. Twele, W. Cao, S. Plank, S. Martinis, Sentinel-1-based flood mapping: a fully automated processing chain, Int. J. Rem. Sens. 37 (13) (2016) 2990–3004, https://doi.org/10.1080/01431161.2016.1192304.
[28] E. Attema, P. Bargellini, P. Edwards, G. Levrini, S. Lokas, L. Moeller, B. Rosich-Tell, P. Secchi, R. Torres, M. Davidson, P. Snoeij, Sentinel-1 the Radar Mission for GMES Operational Land and Sea Services, 2007. https://www.esa.int/esapub/bulletin/bulletin131/bul131a_attema.pdf.
[29] M.A. Łukosz, R. Hejmanowski, W.T. Witkowski, Evaluation of ICEYE microsatellites sensor for surface motion detection – jakobshavn glacier case study, Energies 14 (12) (2021) 3424, https://doi.org/10.3390/en14123424.
[30] A.E. Gaughan, F.R. Stevens, C. Linard, P. Jia, A.J. Tatem, High resolution population distribution maps for southeast asia in 2010 and 2015, PLoS One 8 (2) (2013) e55882, https://doi.org/10.1371/journal.pone.0055882.
[31] R. Soden, L. Palen, From crowdsourced mapping to community mapping: the post-earthquake work of OpenStreetMap Haiti, in: COOP 2014 - Proceedings of the 11th International Conference on the Design of Cooperative Systems, 27-30 May 2014, Nice (France), Springer International Publishing, Cham, 2014, pp. 311–326, https://doi.org/10.1007/978-3-319-06498-7_19.
[32] M. Dittus, G. Quattrone, L. Capra, Mass participation during emergency response: event-centric crowdsourcing in humanitarian mapping, in: Proceedings of the 2017 ACM Conference on Computer Supported Cooperative Work and Social Computing, CSCW '17. Association for Computing Machinery, New York, NY, USA, 2017, pp. 1290–1303, https://doi.org/10.1145/2998181.2998216.
[33] Y. Li, F.B. Osei, T. Hu, A. Stein, Urban flood susceptibility mapping based on social media data in Chengdu city, China, Sustain. Cities Soc. 88 (2023) 1–11, https://doi.org/10.1016/j.scs.2022.104307.
[34] N.N. Patel, E. Angiuli, P. Gamba, A. Gaughan, G. Lisini, F.R. Stevens, A.J. Tatem, G. Trianni, Multitemporal settlement and population mapping from landsat using Google earth engine, Int. J. Appl. Earth Obs. Geoinf. 35 (2015) 199–208, https://doi.org/10.1016/j.jag.2014.09.005.
[35] K. Lechner, M. Gähler, Earth observation based crisis information – emergency mapping services and recent operational developments, in: 4th International Conference on Information and Communication Technologies for Disaster Management, ICT-DM), 2017, pp. 1–7 https://doi.org/10.1109/ICT-DM.2017.8275682, 2017.
[36] Tanzania Urban Resilience Program (Turp), Annual Report, 2022, p. 2022. https://resilienceacademy.ac.tz/wp-content/uploads/2021/04/TURP-Annual-Report-2020.pdf.
[37] Resilience Academy, About Us, 2023. https://resilienceacademy.ac.tz/about-us. 3.1.2023.
[38] H. Aman, P. Irani, F. Amini, Revisiting crisis maps with geo-temporal tag visualization, IEEE Pacific Visualization Symposium (2014), https://doi.org/10.1109/PacificVis.2014.55.
[39] E. Schröter, R. Kiefl, E. Neidhardt, G. Gurczik, C. Dalaff, K. Lechner, Trialing innovative technologies in crisis Management–"Airborne and terrestrial situational awareness" as support tool in flood response, Appl. Sci. 10 (11) (2020) 3743, https://doi.org/10.3390/app10113743.
[40] R. Rydvanskiy, N. Hedley, 3D geovisualization interfaces as flood risk management platforms: capability, potential, and implications for practice, Cartographica 55 (2020) 281–290, https://doi.org/10.3138/cart-2020-0003.
[41] A. Kuveždić Divjak, M. Lapaine, Crisis maps—observed shortcomings and recommendations for improvement, ISPRS Int. J. Geo-Inf. 7 (2018) 436, https://doi.org/10.3390/ijgi7110436.
[42] J. Ardila, P. Laurila, P. Kourkouli, S. Strong, Persistent Monitoring and Mapping of Floods Globally Based on the Iceye Sar Imaging Constellation, IGARSS 2022, https://doi.org/10.1109/IGARSS46834.2022.9883587.
[43] V. Ignatenko, P. Laurila, A. Radius, L. Lamentowski, O. Antropov, D. Muff, ICEYE microsatellite SAR constellation status update: evaluation of first commercial imaging modes, IGARSS 2020 - 2020 IEEE International Geoscience and Remote Sensing Symposium (2020) 3581–3584, https://doi.org/10.1109/IGARSS39084.2020.9324531.
[44] D. Muff, V. Ignatenko, O. Dogan, L. Lamentowski, P. Leprovost, M. Nottingham, A. Radius, T. Seilonen, V. Tolpekin, The ICEYE Constellation - Some New Achievements, *2022 IEEE Radar Conference (RadarConf22)*, 2022, pp. 1–4, https://doi.org/10.1109/RadarConf2248738.2022.9764281.
[45] ICEYE SAR Product Guide (2021) ICEYE 1.5.2021. 21.11.2022.
[46] D. Palacios-Lopez, F. Bachofer, T. Esch, M. Marconcini, K. MacManus, A. Sorichetta, J. Zeidler, S. Dech, A.J. Tatem, P. Reinartz, High-resolution gridded population data sets: exploring the capabilities of the world settlement footprint 2019 imperviousness layer for the african continent, Rem. Sens. 13 (1142) (2021) 1–26, https://doi.org/10.3390/rs13061142.
[47] D. Marks, The urban political ecology of the 2011 floods in Bangkok: the creation of uneven vulnerabilities, Pac. Aff. 88 (3) (2015) 623–651, https://doi.org/10.5509/2015883623.
[48] Z. Raziel, Conagua y Sacmex descargaron e inundaron con aguas negras a Tula; se planeó así para salvar al Valle de México. Animal Politico 11, 2021 10.2021. https://www.animalpolitico.com/2021/11/conagua-sacmex-inundaron-aguas-negras-tula-valle-mexico-cdmx. 27.07.2022.
[49] B. Guillén, El Gobierno reconoce en un informe que la inundación de Tula se debió a la descarga en exceso de agua del Valle de México, 2021 El País 17.10.2021. https://elpais.com/mexico/2021-11-17/el-gobierno-reconoce-en-un-informe-que-la-inundacion-de-tula-se-debio-a-la-descarga-en-exceso-de-agua-del-valle-de-mexico.html. 27.07.2022.
[50] IPCC (2022): Annex I: Global to Regional Atlas [Pörtner, H.-O., A. Alegría, V. Möller, E.S. Poloczanska, K. Mintenbeck, S. Götze (eds.)]. In: Climate Change 2022: Impacts, Adaptation and Vulnerability. Contribution of Working Group II to the Sixth Assessment Report of the Intergovernmental Panel on Climate Change [H.-O. Pörtner, D.C. Roberts, M. Tignor, E.S. Poloczanska, K. Mintenbeck, A. Alegría, M. Craig, S. Langsdorf, S. Löschke, V. Möller, A. Okem, B. Rama (eds.)]. Cambridge University Press, Cambridge, UK and New York, NY, USA, pp. 2875, doi:10.1017/9781009325844.028.
[51] C. Blanchet, Driving Claims Excellence with Technology for Flooding Events, INSTECH London, 2021. https://www.instech.co/sites/default/files/driving-claims-excellence-technology-flooding-events-report.pdf. 20.7.2023.
[52] S.K.V. Vanama, D. Mandal, Y.S. Rao, GEE4FLOOD: rapid mapping of flood areas using temporal Sentinel-1 SAR images with Google Earth Engine cloud platform, J. Appl. Remote Sens. 14 (3) (2020), https://doi.org/10.1117/1.JRS.14.034505.
[53] ICEYE Product Documentation, The ICEYE Fleet, 26.07, 2022 2022. https://iceye-ltd.github.io/product-documentation/5.0/productguide/fleet.
[54] M. Marconcini, A. Metz-Marconcini, S. Üreyen, D. Palacios-Lopez, W. Hanke, F. Bachofer, J. Zeidler, T. Esch, N. Gorelick, A. Kakarla, M. Paganini, E. Strano, Outlining where humans live, the world settlement footprint 2015, Sci. Data 7 (1) (2020) 242, https://doi.org/10.1038/s41597-020-00580-5.

[55] A.Y. Grinberger, M. Minghini, L. Juhász, G. Yeboah, P. Mooney, OSM science – the academic study of the OpenStreetMap project, data, contributors, community, and applications, International Journal of Geo-Information 11 (4) (2022) 1–230, https://doi.org/10.3390/ijgi11040230.
[56] L. Palen, R. Soden, T.J. Anderson, M. Barrenechea, Success & scale in a data-producing organization: the socio-technical evolution of OpenStreetMap in response to humanitarian events, in: Proceedings of the 33rd Annual ACM Conference on Human Factors in Computing Systems, CHI '15, Association for Computing Machinery, New York, NY, USA, 2015, pp. 4113–4122, https://doi.org/10.1145/2702123.2702294.
[57] J. Anderson, D. Sarkar, L. Palen, Corporate editors in the evolving landscape of OpenStreetMap, International Journal of Geo-Information 8 (5) (2019) 232–250, https://doi.org/10.3390/ijgi8050232.
[58] R.S.M. Hernaiz, Enhancing geospatial preparedness for disaster management through the work of development organisations, in: Doctoral Thesis in Information Management, NOVA Information Management School, Universidade Nova de Lisboa, 2019. https://run.unl.pt/bitstream/10362/98700/1/D0055.pdf.
[59] OpenStreetMap, Who uses OpenStreetMap? https://welcome.openstreetmap.org/about-osm-community/consumers, 2022, 04.08.2022.
[60] G. Boeing, OSMnx: new methods for acquiring, constructing, analyzing, and visualizing complex Street networks, Comput. Environ. Urban Syst. 65 (2017) 126–139, https://doi.org/10.1016/j.compenvurbsys.2017.05.004.
[61] A. Erman, M. Tariverdi, M. Obolensky, X. Chen, R.C. Vincent, S. Malgioglio, J. Rentschler, S. Hallegatte, N. Yoshida, Wading out the storm: the role of poverty in exposure, vulnerability and resilience to floods in dar es Salaam, Policy Research Working Paper 8976 (2019)1–50.
[62] A. Pistrika, G. Tsakiris, I. Nalbantis, Flood depth-damage functions for built environment, Environmental Processes 1 (2014) 553–572, https://doi.org/10.1007/s40710-014-0038-2.
[63] J. Huizinga, H. de Moel, W. Szewczyk, Global flood depth-damage fuctions: methodology and the database guidelines, Joint Research Center (JRC) Technical Report 1–110 (2017) https://doi.org/10.12760/16510, EUR 28552.
[64] H.R. Wallingford, R&D Outputs, Flood Risks to People: Phase 2 FD2321/TR2 – Guidance Document, Defra/Environmental Agency, Flood and Coastal Defence R&D Programme, 2006, pp. 1–91. https://www.gov.uk/flood-and-coastal-erosion-risk-management-research-reports/flood-risks-to-people-phase-2-managing-risks-and-dangers%2027.07.2022.
[65] Kepler gl, 2022. https://docs.kepler.gl. 04.08.2022.
[66] ICEYE, Breaking the 15 Minute Barrier from Acquisition to Delivery for SAR Imaging, vol. 7, 2023 6.2023. https://www.iceye.com/press/press-releases/iceye-ksat-announce-ground-segment-15-minute-tasking-to-processing-sar-image-capabilities. 12.8.2023.
[67] UNITAR, Independent Evaluation of UNOSAT Rapid Mapping Service – Final Report, 2018. https://unitar.org/sites/default/files/media/file/independent_evaluation_of_unosat_rapid_mapping_service_final_report.pdf. 23.01.2023.
[68] Copernicus Emergency Management Service, Rapid Mapping, 2022. https://emergency.copernicus.eu/mapping/ems/rapid-mapping-portfolio. 23.01.2023.
[69] Y.-K. Lee, S.-H. Hong, S.-W. Kim, Monitoring of water level change in a dam from high-resolution SAR data, Rem. Sens. 13 (18) (2021) 3641, https://doi.org/10.3390/rs13183641.
[70] T. Barreto, J. Almeida, F. Cappabianco, Estimating accurate water levels for rivers and reservoirs by using SAR products: a multitemporal analysis, Pattern Recogn. Lett. 83 (2016), https://doi.org/10.1016/j.patrec.2016.05.015.
[71] X. Zheng, D.R. Maidment, D.G. Tarboton, Y.Y. Liu, P. Passalacqua, GeoFlood: large-scale flood inundation mapping based on high-resolution terrain analysis, Water Resour. Res. 54 (2018) https://doi.org/10.1029/2018WR023457, 10,013–10,033.
[72] J. Hofmann, H. Schüttrumpf, floodGAN: using deep adversarial learning to predict pluvial flooding in real time, Water 13 (2021) 2255, https://doi.org/10.3390/w13162255.
[73] A. Yao, A. Crooks, B. Jiang, J. Krisp, Xintao Liu, H. Huang, Deploying geospatial visualization dashboards to combat the socioeconomic impacts of COVID-19, Environ. Plan. B Urban Anal. City Sci. 1262–1279 50 (5) (2023), https://doi.org/10.1177/23998083221142863.